https://doi.org/10.5194/egusphere-2024-2744
Preprint. Discussion started: 3 April 2025

An Assessment of Antarctic Sea-ice Thickness in CMIP6 Simulations with Comparison to the Satellite-based Observations and Reanalyses

Shreya Trivedi[1], Will Hobbs[2], and Marilyn Raphael[1]

[1]Department of Geography, University of California, Los Angeles

[2]Australian Antarctic Program Partnership, Institute for Marine and Antarctic Studies, University of Tasmania, nipaluna/Hobart, Australia

Corresponding author: Shreya Trivedi (shreyatrivedi26@ucla.edu)

https://doi.org/10.5194/egusphere-2024-2744
Preprint. Discussion started: 3 April 2025

Abstract

Sea-ice thickness, though critical to our understanding of sea-ice variability, remains relatively understudied compared to surface sea-ice parameters in the Southern Ocean. To remedy this, we examine spatio-temporal variations in sea-ice thickness by analyzing historical simulations from 39 coupled climate models in CMIP6, comparing them with three sea-ice products, including satellite-derived observations and reanalyses. Furthermore, we compare seasonal trends in simulated sea ice thickness with trends in sea ice area. Our results indicate that CMIP6 models can replicate the mean seasonal cycle and spatial patterns of sea-ice thickness. During its maximum in February, these models align well with satellite-based observation products. However, during the annual minima, CMIP6 models show significant agreement with the reanalysis products. Certain models exhibit unrealistic historical mean states compared to the sea-ice products resulting in significant inter-model spread. CMIP6 models can simulate sea-ice area more accurately than the sea-ice thickness. They also simulate a positive relationship between the two parameters in September such that models with greater area tend to exhibit thicker ice. In contrast, there is a negative relationship in February when greater area is associated with lower thickness since only the thicker ice survives the summer melt. Moreover, our study highlights significant positive trends in sea-ice thickness observed during the cooler seasons, which are nearly absent in the warmer seasons where positive trends are predominantly observed in sea-ice area. The spatial distribution of SIT biases is closely linked to uncertainties in modeling the ice edge and the dynamic processes, emphasizing the need for better model representation of both. This study, therefore, highlights the need for improved representation of Antarctic sea-ice processes in models for accurate projections of thickness and related volume changes.

1. Introduction

Antarctic sea-ice extent which showed a small positive linear trend since the start of the satellite era (Cavalieri & Parkinson, 2008; Parkinson & Cavalieri, 2012; Turner et al., 2015; Zwally et al., 2002), has decreased significantly since mid-2015 (Raphael and Handcock, 2022; Wang et al., 2022; Turner et al., 2022; Eayrs et al., 2021). Since there is a long and reliable observational record available for the surface characteristics (such as extent and area) of the ice, they have been the primary focus for understanding the variability in the sea-ice cover in the Antarctic. However, complete understanding of the changes in sea-ice and their potential impact on climate (*via* a variety of climate-sea-ice feedbacks) and marine ecosystems is not possible without an understanding of the variability in sea-ice thickness (SIT) and volume (SIV) (Holland et al., 2006; Stammerjohn et al., 2008).

SIV (*viz.* the product of both area and thickness) serves as a measure of total sea-ice production and, hence, a measure of the surface salinity flux in winter, the freshwater input to the ocean in summer, and total heat exchange with the atmosphere (Maksym et al., 2012). Understanding the variability in SIV improves our understanding of surface buoyancy flux and its impact on the ventilation of Southern Ocean deep waters, as well as trends and variability in salinity in the region (Haumann et al., 2016; Abernathy et al, 2016; Pellichero et al., 2018). This understanding in turn, informs our knowledge about global ocean heat and carbon uptake processes (Williams et al., 2023).

https://doi.org/10.5194/egusphere-2024-2744
Preprint. Discussion started: 3 April 2025

SIT varies seasonally and is an important component of the Antarctic ice budget (Kurtz & Markus, 2012; Worby et al., 2008). SIT is important for the marine biology of the Antarctic ecosystem. It affects the maximum biomass of algae in different ice layers, which in turn influences the food web of the Southern Ocean. SIT, along with the snow depth, affects the light penetration and availability for the phytoplankton contributing further to their production and bloom (Massom & Stammerjohn, 2010; Schultz, 2013). Therefore, a long-term assessment of SIT/SIV in combination with surface sea-ice characteristics, is important for a complete understanding of the ongoing changes in the Antarctic sea-ice and its impacts (Massonnet et al., 2013; Sallée et al., 2023).

Among the currently available SIT datasets, ship-based observations from ASPeCt (Antarctic Sea ice Processes and Climate) tend to underestimate mean measurements because ship routings preferably avoid thicker sea-ice (Worby et al., 2008). Airborne electromagnetic data, NASA Operation *IceBridge* (Koenig et al., 2010) and the upward-looking sonars (ULS) (Behrendt et al., 2013) provide valuable spatio-temporal information but are limited to certain regions, lacking circum-Antarctic distribution. To overcome some of the limitations, advanced retrieval techniques in the form of satellite remote sensing, including passive microwave sensors for thin ice (Kurtz & Markus, 2012), and active sensors like Synthetic Aperture Radar (SAR), have now been applied to study circum-Antarctic SIT coverage and its long-term trends. More recently published satellite-derived (both radar from Envisat-CryoSat-2 and laser from ICESat-2) altimetry-based SIT datasets have proven to be the best source for circum-Antarctic SIT retrievals over the full thickness range (Kurtz and Markus, 2012; Kacimi and Kwok, 2020; Wang et al., 2022). In general, gathering Antarctic SIT data presents significant challenges owing to harsh weather conditions, extensive snow cover, and intricate snow metamorphism processes. These factors introduce uncertainties in both *in-situ* measurements and satellite altimetry observations, particularly concerning the accuracy of detecting the snow-ice interface in the latter method. *In-situ* measurements like drilling data are accurate but extremely limited in time and space and suffer from biases. We discuss such uncertainties in detail in Sect.2.1.

Given the inconsistencies and limitations in the existing SIT observations, Global Coupled Climate Models (GCMs) can serve as potentially valuable tools for assessing long-term SIT/SIV variability and providing future projections. Hou et al. (2024) compared SIT simulations in CMIP6 models with radar altimetric datasets (Envisat-CryoSat-2) and identified common issues, including lags and significant underestimation in SIT climatology during autumn and winter months, as well as negative biases, particularly in the sea ice deformation zone around Antarctica. Assessment of the accuracy of SIT simulations in GCMs remains a challenge, which adds to the *low confidence* in Antarctic sea-ice projections (Meredith et al, 2019). This gap underscores the need for further research, which is a key motivation for our study.

In this study, we present a high-level evaluation of models in the Sixth Coupled Model Intercomparison Project (CMIP6; Eyring et al., 2016) which simulate Antarctic SIT. We compare these simulations to three different sea-ice products, including radar altimetric (as in Hou et al., 2024) as well as two reanalysis (synthesis) datasets. Our results indicate that CMIP6 models can reasonably capture the timing of the annual cycle and the spatial patterns in SIT, albeit with some biases and model disagreements. However, when compared to sea-ice area (SIA), the models' performance remains suboptimal. This underscores the need for further improvements in the representation of sea-ice dynamics and the physical processes controlling sea-ice-ocean interactions in GCMs.

https://doi.org/10.5194/egusphere-2024-2744
Preprint. Discussion started: 3 April 2025

Since our understanding of historical sea-ice variability and the evaluation of climate models has traditionally relied heavily on SIA records, this study extends the analysis by comparing simulated SIT and SIV to SIA, in order to see how these diagnostics are related. Furthermore, we examine the inter-relations between SIT and SIA during two key months to better understand their covariability. We also identify significant seasonal trends in the three sea-ice parameters and analyze their evolution over the selected time-period. These results emphasize the importance of incorporating SIT metrics into future model evaluations to enhance our understanding of Antarctic sea-ice dynamics and improve sea-ice and climate projections.

2. Data and Methods

2.1 Sea-ice products

Our study uses three different sea-ice records for SIT (Table S1): A dataset derived from Envisat-CryoSat-2 (2002-2017; henceforth referred to as satellite product), the Global Ice-Ocean Modeling and Assimilation System (GIOMAS, 1979-2014) and the German contribution to the Estimating the Circulation and Climate of the Ocean project Version 3 (GECCO3, 1979-2014). We compare them with the CMIP6 *historical* simulations which run until 2014. Since the satellite products do not begin before 2002, our study focuses on the time-period between 2002-2014. SIA is calculated as the product of the monthly values of sea-ice concentration and the grid cell area from the reanalysis dataset, National Snow and Ice Data Center (NSIDC) (Comiso, 2017). SIV is the product of the actual floe thickness, sea-ice concentration and the grid cell area of the respective datasets. In the case of the satellite products, we utilize sea-ice concentration values from the NSIDC.

SIT from Satellite Altimetry- Envisat and CryoSat-2:

The Sea-Ice Climate Change Initiative (SICCI) project provides a large-scale Antarctic SIT dataset from Envisat and CryoSat-2 with a 50 km spatial resolution (Hendricks et al., 2018a, 2018b). Both Envisat and CryoSat-2 carry a radar altimeter based on the Ku Band frequency which is expected to measure the ice freeboard (total freeboard minus snow depth), with spatiotemporal resolution and spatial coverage consistent with each other. Our study utilizes the aggregated time-series data from both satellites owing to the reasonable alignment of mean and modal values derived from their radar freeboards throughout the sea-ice seasons (Hou et al., 2024; Schwegmann et al., 2016). The SICCI dataset stands out as the most comprehensive satellite dataset spanning the circum-Antarctic SIT from 2002 to present (Shi et al., 2021, Hou et al., 2024). This coverage is not matched by more recent datasets like ICESat-2 (Xu et al., 2021). It is comparable to ULS-derived SIT for the Weddell region (Shi et al., 2021; Liao et al., 2022; Wang et al., 2022) and aligns well with *in-situ* ship-based observations (ASPeCt; Worby et al., 2008), showing highest thickness in summers and lowest in autumn-winter.

Retrieval of such Antarctic SIT products is quite challenging and the existing satellite datasets are not without uncertainties. Although the altimetric SIT measurements of Envisat and CryoSat-2 observations represent a major advancement in monitoring Antarctic SIT, it is an experimental climate data record with uncertainties resulting from the inaccuracy in determining the snow–ice interface (Willatt et al., 2010) and biases due to surface-type mixing and surface roughness (Schwegmann et al., 2016; Paul et al., 2018; Tilling et al., 2019) resulting in overestimations (Hendricks et al., 2018a, b; Shi et al., 2021; Wang et al., 2022).

https://doi.org/10.5194/egusphere-2024-2744
Preprint. Discussion started: 3 April 2025

SIT from Reanalysis/Synthesis products:

Reanalyses integrate information from observations and ocean-sea-ice models through data assimilation and provide gridded sea-ice data with homogeneous spatiotemporal sampling over an extended time-period. The use of ocean–sea-ice models forced by atmospheric reanalysis is a general approach to better constrain SIT changes with the observations, in both the Arctic and Antarctic. Since the reanalysis datasets offer state estimations closer to observations compared to model-only data, it makes them a valuable tool in Antarctic sea-ice studies (Kumar et al., 2017). Hence, our study uses two such estimates of long-term Antarctic SIT changes and compares them against the satellite products and the GCMs.

GECCO3 ocean synthesis is an improved version of GECCO2 based on MITgcm which employs the adjoint method to fit the model to a large variety of data over a multidecadal period (1948-2018). GECCO3 has 40 levels and uses the horizontal and vertical grid of the ocean component of MPI-ESM in the MR/HR configuration, providing a global eddy-permitting synthesis at a nominal resolution of 0.4° (Köhl, 2020). GIOMAS uses the Parallel Ocean Model coupled with a 12-category thickness and enthalpy distribution ice model at a horizontal resolution of 0.8° (Zhang & Rothrock, 2003). GIOMAS assimilates sea-ice concentration, demonstrates good agreement of its SIT with satellite observations in the Arctic (Lindsay & Zhang 2006) and is useful for studying long-term variations in Antarctic sea-ice (Liao et al., 2022; Shi et al., 2021). To make the GECCO3 and GIOMAS products comparable to absolute floe thickness estimates (the SIV per grid-cell area or "equivalent sea-ice thickness"), we convert them into "effective thicknesses" by dividing them by their respective sea-ice concentration records.

2.2 CMIP6 Models

We analyze the *historical* experiments of the CMIP6 dataset, specifically focusing on the *sithick* variable, which represents simulated effective or actual floe thickness. We also use *siconc* (sea-ice concentration) and *areacello* (area of individual grid cells over the ocean) variables. CMIP6 models generate multiple ensemble members, which are multiple runs or simulations with slightly different initial conditions or parameter settings, used to capture uncertainty and variability in model predictions. In this study, we consider a single ensemble for each model (Table S2) to account for internal variability and ensure fairness by not giving weight to the models with multiple ensemble members (following Notz & Community, 2020; Roach et al., 2020). We calculate SIV by multiplying *siconc*, *sithick* and *areacello* and summing over the circum-Antarctic Southern Ocean. For SIA, we calculate the area integral product of *siconc* and *areacello*. Lastly, for floe thickness, we use the averaged *sithick* over the Southern Ocean. The multi-model means (MMM) are calculated based on the single ensemble member in 39 coupled climate models for all the three sea-ice variables.

3. Results

3.1 Mean and Anomaly State

This section first discusses the mean annual cycles of SIA, SIV and SIT for the different sea-ice products and the CMIP6 models over the period of 2002-2014 (Fig.1). It then examines the biases and spreads in the climate models and, finally, the simulated and observed seasonal trends in the anomalies across all the sea-ice variables.

https://doi.org/10.5194/egusphere-2024-2744
Preprint. Discussion started: 3 April 2025

Fig.1a highlights that all the sea-ice products agree on the timing of their SIA maxima and minima (in September and February, respectively). However, GIOMAS, despite having the same maximum and minimum timings, exhibits a lower amplitude, particularly during the winter season. All the CMIP6 models similarly simulate the observed timing of maxima and minima in SIA, however the MMM remains consistently lower than all other sea-ice products throughout the year. Overall, significant negative biases are observed in the simulated SIA cycles, except for a few models that consistently simulate larger SIAs throughout the year.

For the SIV, all the sea-ice products display pronounced annual cycles (Fig.1b). While their minima are similar in timing and magnitude, their maxima do not occur at the same time, with the satellite products showing the earliest maxima and GECCO3 the latest. Additionally, the amplitudes of the SIV cycles are highest in the satellite products and lowest in GECCO3. All the CMIP6 models simulate a similar annual cycle to the sea-ice products, with their MMM maxima in October and minima in March (lagging the sea-ice products by one month). Like SIA, the MMM SIV is biased low compared to all the sea-ice products, agreeing best with GECCO3.

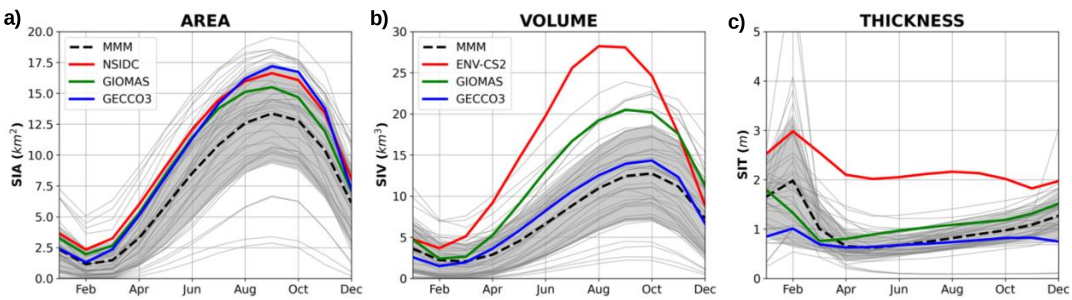

Figure 1: Comparison of annual cycles of SIV, SIT and SIA of the circumpolar Antarctic. All the CMIP6 models are shown as grey lines, The Multi-Model Mean (MMM) is the black dashed line. GECCO3 in blue, GIOMASS in green, and Envisat-CryoSat-2/NSIDC in red. Grey shaded areas are +-1 standard deviation for the MMM. Scale: million km^2 and thousand km^3.

Fig.1c shows that SIT has a different annual cycle than SIA and SIV. Its maximum occurs in February, which is observed across all the sea-ice products, except for GIOMAS, where the sea-ice maximum occurs one month earlier. The timing of the SIT minimum is more variable. For the synthesis products, the SIT minimum occurs at the beginning of the growth season, whereas for the satellite products it occurs during the retreating season. CMIP6 models can capture the thickness maxima in February and agree with the synthesis products in showing minima in the fall. However, there is considerable spread in the exact timing of the minimum, with the MMM minimum occurring in May, lagging the reanalysis products. Most of the models simulate thicker sea-ice than the three sea-ice products during summer (between January-April) resulting in biases which considerably decrease for the synthesis products and increase for satellite datasets starting in May. A few models, namely the IPSL and EC-Earth3-models (characterized by significant warm Southern Ocean biases; Döscher et al., 2022), exhibit anomalously thick sea-ice (>3m) in February. On the contrary, CNRM-models exhibit anomalously low thickness throughout the year. This is primarily due to high negative biases in their sea-ice concentration simulations and their inability to

https://doi.org/10.5194/egusphere-2024-2744
Preprint. Discussion started: 3 April 2025

realistically simulate thick sea-ice during the austral summer in the Weddell Sea (Voldoire et al., 2019). These differences can be attributed to various factors, including the multiyear sea-ice surviving the summer melt (Worby et al., 2008), challenges associated with satellite retrieval of summer SIT (Kurtz and Markus, 2012), and the influence of dynamical wind patterns in CMIP6 models, resulting in excessive ridging (Lie et al., 2021).

Summer maxima in SIT vary between January and February depending on the sea-ice product used (Fig.1c). Such high SIT values during summer stand in contrast with the annual minima observed in other sea-ice variables. This SIT annual cycle results from the melt of first year ice in large areas in the seasonal ice zone so that only the thickest ice survives. In the beginning of the freezing season, large areas are covered by newly formed first year ice, which reduces the mean freeboard compared to summer values (Schwegmann et al., 2016). Therefore, the highest average thickness in February is due to the compacted ice which survives the melt season (Kurtz & Markus, 2012; Worby et al., 2008; Xu et al., 2021). It is for this reason that the SIT seasonal cycles look very different from those of SIA or SIV. Therefore, to capture the sea-ice seasons based exclusively on the annual cycle of SIT, we conducted the analyses in Sect. 3.2 and 3.3 using February and September.

The inter-model agreement also varies considerably between seasons and across variables. The inter-model spread of annual mean Antarctic SIT, SIV and SIA is 5.9 m, 20 thousand km^3 and 16 million km^2 for the maxima and 1.8 m, 7.5 thousand km^3 and 4 million km^2 for the minima, respectively. Fluctuations in the inter-model spread are larger during fall and winter for SIV and SIA but shrinks during summers. By contrast, SIT has greater inter-model spread during summer and shrinks significantly from April-November. Notably, for most parts of the year, the inter-model spread in SIT remains smaller than disagreements within the sea-ice products, owing to the overestimations in satellite product during the winter months.

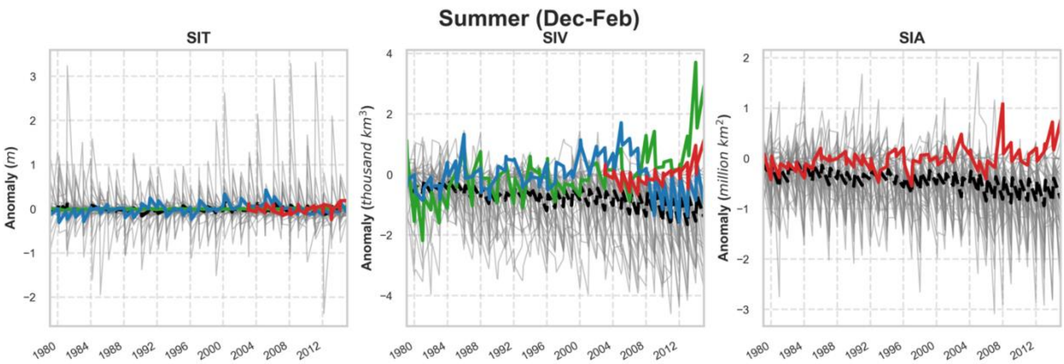

https://doi.org/10.5194/egusphere-2024-2744
Preprint. Discussion started: 3 April 2025

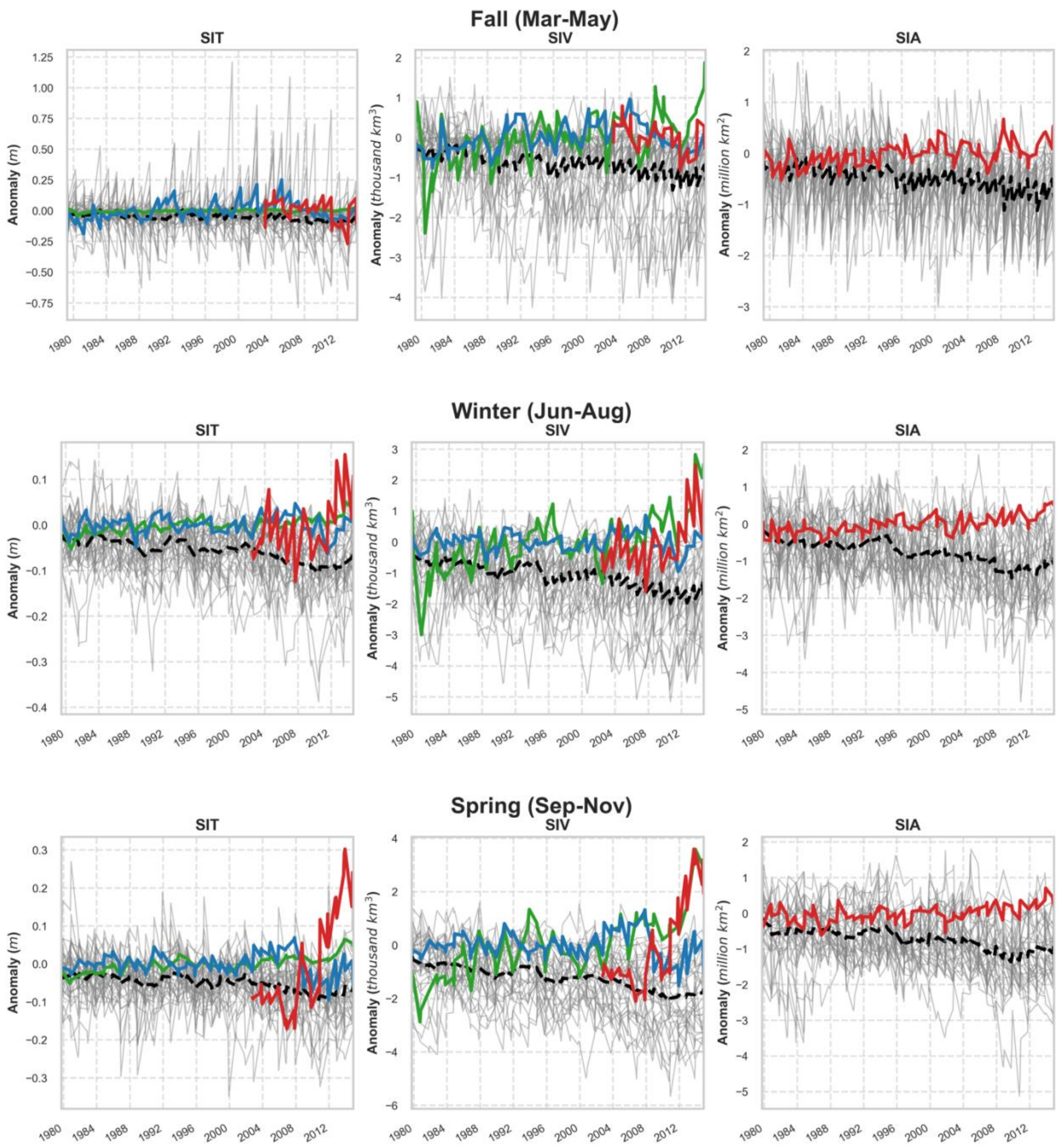

Figure 2: Anomalies for four seasons: Spring and Winter (Cold Seasons), Summer and Fall (Warm Seasons) of SIT (left), SIV (middle) and SIA (right) of the circumpolar Antarctic (1979-2014). All the CMIP6 models are shown as grey lines, Multi-model mean in dashed line, GECCO3 in blue, GIOMASS in green, and Envisat-CS-2/NSIDC in red.

Next, we look at the seasonal trends in the anomalies of the three sea-ice variables across different CMIP6 models and the sea-ice products. In general, CMIP6 models simulate negative trends in Antarctic SIA and extent (Roach et al., 2020 and Shu et al., 2020), contrasting with the observed positive trend until mid-2015 (Li et al., 2023; Shu et al., 2015; Turner et al., 2013). Figure 2 demonstrates a similar pattern in the simulated SIT/SIV with a negative trend noticed across all

https://doi.org/10.5194/egusphere-2024-2744
Preprint. Discussion started: 3 April 2025

the sea-ice variables. However, there exists a difference in trends for different seasons across different sea-ice products starting in the early 2000s. There are significant positive trends in SIT/SIV observed during the cooler seasons (winter and spring), while such trends are absent in the warmer seasons. Note that studies have shown that small positive SIA trends (during the time-period of 1979-2014) are primarily observed in the warmer seasons (Summer and Fall) while they are reduced during the cooler seasons as the maximum ice edge is thermodynamically constrained by the Southern Ocean polar front (Martinson, 2012; Eayrs et al., 2019). This implies that changes in Antarctic SIT may contribute to the variability in total sea-ice mass/volume during colder months. The presence of robust land-ocean temperature gradients during winters may be a contributing mechanism here because they result in high-intensity winds, which are recognized as one of the significant contributors to SIT/SIV fluctuations in the Southern Ocean (Zhang, 2014).

3.2 Seasonal Variations and Inter-relationships

An accurate spatio-temporal distribution of SIT is key to accurate estimates of SIA and eventually SIV distributions. It reflects the skill in simulation of local processes, coupled interactions and energy transfer among the ocean below, the sea-ice, and the atmosphere above (Stroeve et al., 2014). To estimate seasonal variations and evaluate the performance of the CMIP6 models in capturing the observed distribution of sea-ice variables, we plot the Taylor Diagrams (Fig.3) representing the spatial correlation coefficients, Root Mean Square Deviation (RMSD; not shown in the Figure but included in Tables S3-S5) and standard deviation among 39 models, and the three sea-ice products. These calculations were performed based on area-integrated spatial averages of SIT, SIV and SIA over the circum-Antarctic for February and September. We use the satellite dataset as the observation reference for calculating RMSDs and correlation values across the grids.

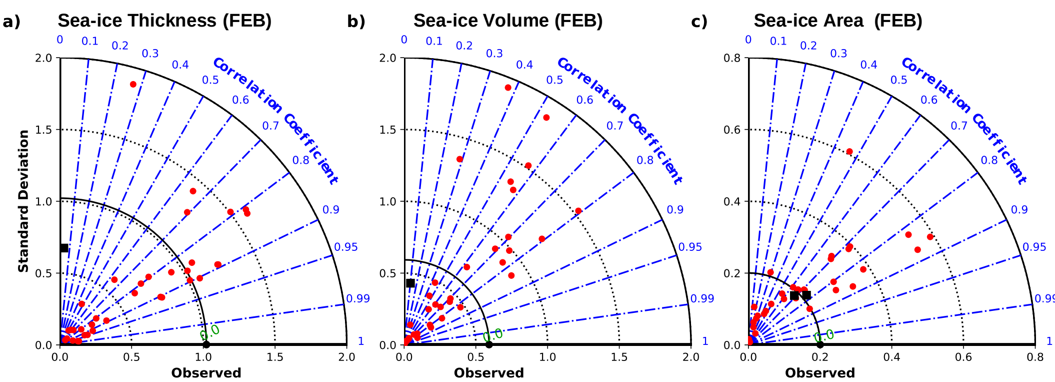

https://doi.org/10.5194/egusphere-2024-2744
Preprint. Discussion started: 3 April 2025

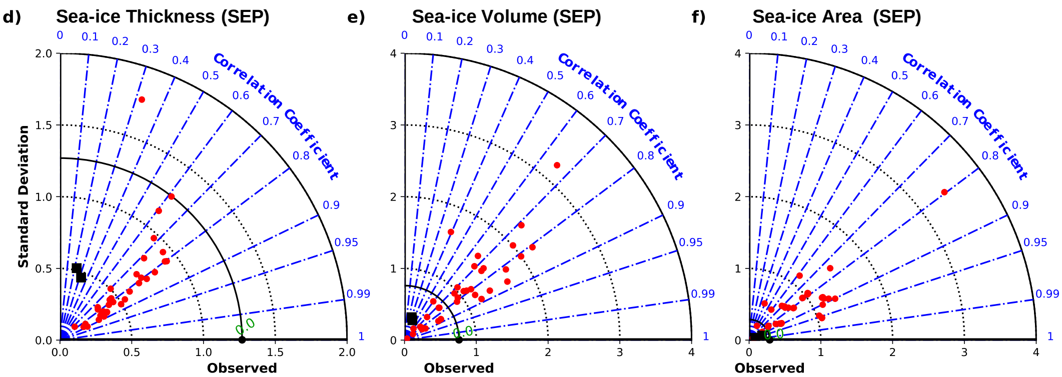

Figure 3: Taylor Diagrams representing spatial correlation and standard deviation using time-averaged means between CMIP6 models and different sea-ice products. For each model and synthesis product, two statistics are plotted: the Pearson correlation coefficient, related to the azimuthal angle (blue contours); and the standard deviation viz proportional to the radial distance from the origin (black dotted contours). Black solid contour corresponds to the standard deviation of the reference dataset. Red dots represent individual CMIP6 models and black squares represent synthesis datasets. The period used for comparison is 2002-2014 for February (a,b,c) and September (d,e,f). For February (a and b), GECCO3 is not included as it had very small negative correlation coefficients. Reference datasets used for SIT and SIA are Envisat-CryoSat-2 and NSIDC, respectively. Higher correlation coupled with a lower RMSD indicates greater accuracy of CMIP6 models in simulating the sea-ice variables.

The correlation coefficients in Fig.3 range between 0.6-0.9 for all the variables in both the months (Tables S3, S4 and S5). Specifically, models tend to exhibit the highest variability in SIT, as indicated by higher RMSDs and standard deviation values that deviate significantly from those of the reference dataset (Fig.3a,d). Both synthesis products (GIOMAS and GECCO3) show the highest variability and lowest correlations for SIT, indicating lack of agreement among different sea-ice products. Whereas the opposite is observed for SIA where most of the models and reanalysis products have a lower variability for SIA (Fig.3c,f) compared to SIV and SIT. When comparing the two months, lower variability and higher correlations are observed for all the sea-ice variables in February (Fig.3a-c). In summary, the Taylor Diagram reveals that while most CMIP6 models demonstrate higher accuracy in simulating SIA and SIV (with high correlations and low RMSDs), their SIT simulations are less accurate. The widely spread standard deviations suggest considerable differences in how the models simulate internal variability in SIT, highlighting their underlying uncertainties in representing such variability. There also exists a disparity in their seasonal accuracy with models performing better during February across all the variables.

https://doi.org/10.5194/egusphere-2024-2744
Preprint. Discussion started: 3 April 2025

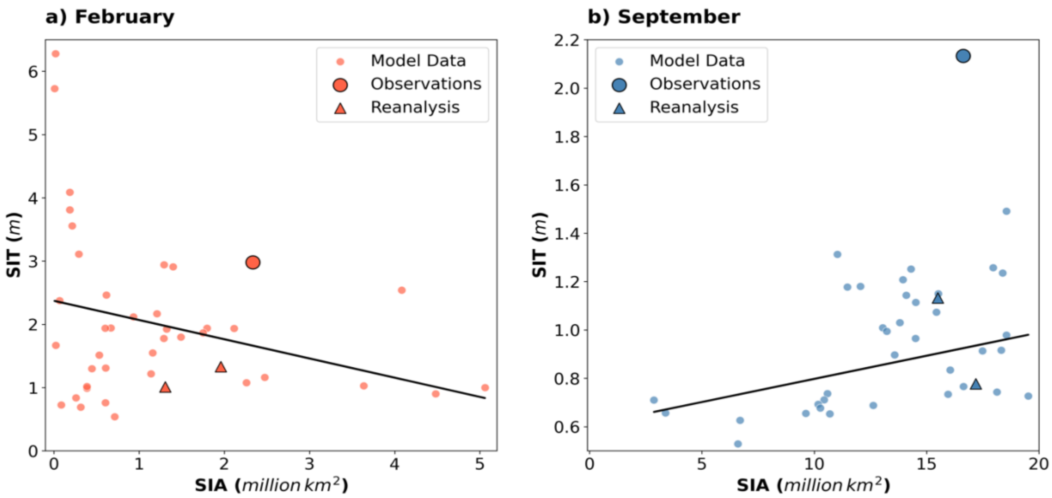

Figure 4: Scatter plots between the climatological means of SIT (y-axis) and SIA (x-axis) for CMIP6 models and Observations for the period (2002-2014) for February (red) and September (blue). The line of best fit represents the relationship between the two variables for selected months. Each small dot represents a model while the larger dots represent observations (Envisat-CryoSat-2 and NSIDC for SIT and SIA, respectively). The reanalysis/synthesis datasets are represented by triangles. The figure clearly demonstrates seasonal variations in magnitudes of both the variables.

Given their better performance in simulating SIA, we further investigate whether or not this performance is correlated with SIT accuracy in individual CMIP6 models and the synthesis products. This evaluation has not been done before; however, examining this interrelationship will significantly enhance our understanding of sea-ice changes, which has so far been largely based on surface parameters such as SIA. Additionally, it will provide deeper insights into the interpretation of existing historical records of surface sea-ice parameters in the Antarctic. For this, we compare the annual averages of SIT and SIA in models and the synthesis products using the satellite product as the observational reference (Fig.4). The comparison shows that SIA biases range between -2 to 2 million km^2 during February and between -14 to 4 million km^2 during September. In February, although SIT is at maximum, most models simulate thinner sea-ice with values below the satellite estimates of 3m. During September, the models consistently show thin biases with values ranging between 1-2m across all the models.

Figure 4 also highlights how simulated SIA and SIT are differently related depending on the time of year (also evident in Fig.2). In summer, SIA and SIT biases are negatively correlated (Fig.4a; although we note that many models have very low SIA in February), and in winter they are positively correlated (Fig.4b). One possible way to explain this is that models with strong melt seasons result in low summer sea-ice cover in which only the thickest ice can survive. The reverse may be true for weaker melt seasons which may allow more, and thinner, ice to survive, leading to greater SIA made up of thinner ice. In winter, greater sea-ice freezing will lead to both thicker ice and a larger area, explaining the positive relationship between the SIA and SIT biases in Fig.4b. This contrasting seasonal relationship raises questions about whether SIA is a reliable predictor of

https://doi.org/10.5194/egusphere-2024-2744
Preprint. Discussion started: 3 April 2025

SIT, which has significant implications for our understanding of sea-ice changes when based solely on SIA. Further studies are needed to clarify this.

3.3 Seasonality in SIT Biases

This section investigates the seasonality in SIT biases in both temporal and spatial dimensions across three sea-ice products, relative to the multi-model means (MMM) of the selected 39 CMIP6 models. Figure 5 highlights the seasonality in SIT biases, showing patterns in biases with reference to the climatological SIT means across different months and sea-ice products. With respect to the satellite product, most models exhibit negative biases across all months, with the largest bias observed in March. For the two reanalysis/synthesis datasets, the simulated SIT MMM values, except for the February maxima, remain closer to the zero line (within the range of ±0.3m), indicating much smaller biases.

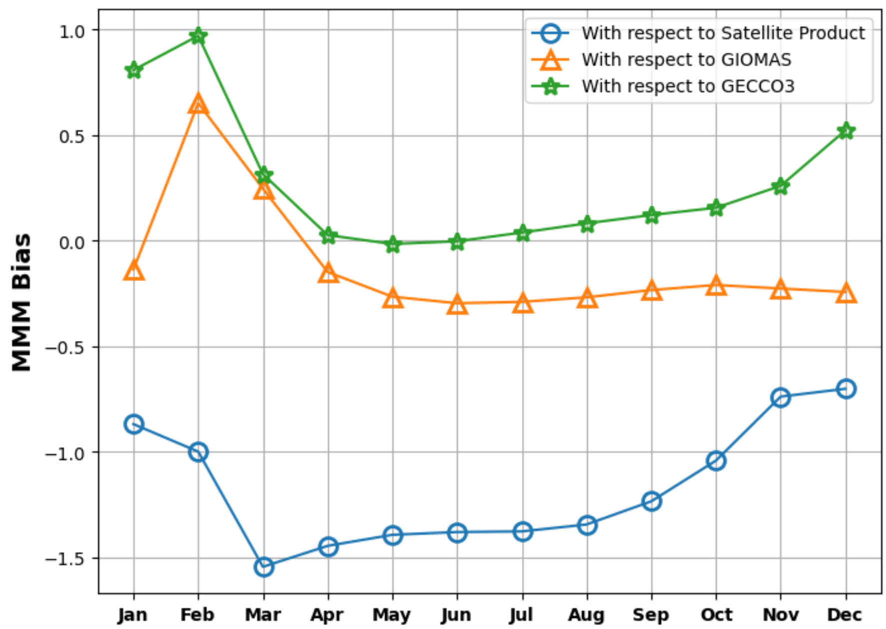

Figure 5: Seasonality in SIT biases (m) calculated as the difference between climatological means of MMM of 39 CMIP6 models and the three sea-ice products (2002-2014).

This section further explores the spatial spread (measured by the standard deviation of the ensemble) in SIT and SIC biases, using three different sea-ice products for February (Fig.6) and September (Fig.7) over the period 2002-2014. In February, higher standard deviations are evident in the Amundsen-Bellingshausen Seas (ABS) and along the coastal edges of the Weddell Sea (blue shaded regions in Fig 6a), indicating greater model disagreement when compared to the sea-ice products during this month. These regional disagreements may result from dynamic processes such as sea-ice drift, melting, and freezing which are not accurately captured by the models. However,

https://doi.org/10.5194/egusphere-2024-2744
Preprint. Discussion started: 3 April 2025

models generally show better alignment with reanalysis/synthesis products in February, as seen in the lower standard deviation values (shown in red), indicating improved agreement.

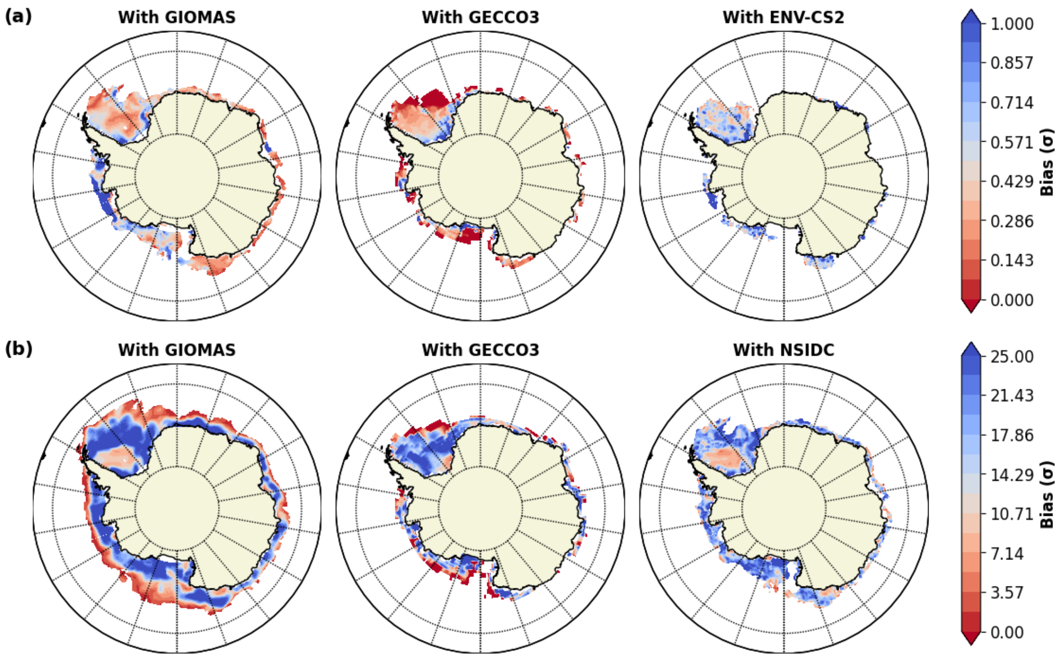

Figure 6: Variability of the Spatial Biases in CMIP6 Models (calculated as Standard Deviation of the difference between CMIP6 MMM and the three distinct sea ice products); for the month of February in (a) SIT (m) and (b) SIC (%).

In contrast to SIT, the spatial bias spread in SIC is larger (Fig.6b), but the pattern remains similar—better model agreement (lower standard deviations) at the ice edges and in the inner Weddell Sea, while there exists poorer agreement (higher standard deviations) closer to the coasts. Figure 6b also helps to determine how SIC biases may contribute to standard deviations observed in the SIT biases. For instance, the regions of higher model disagreements in SIT that coincide with the high SIC standard deviations suggest that model errors in locating the ice edge may also influence the spread of actual thickness and vice versa. Therefore, when models misplace the ice edge, they might overestimate or underestimate SIT in those regions. In February, the model disagreements in the SIT biases near the ABS and the coastal edges of the Weddell (blue regions in Fig.6a) coincide with higher standard deviation values in SIC bias spread (Fig.6b) in the same regions, especially along the southern Weddell coast. This suggests that some of the SIT biases in these regions could be a result of misrepresentation of the ice edge in models, rather than true variations in actual thickness.

In September, there is an overall lower bias spread in SIT across most of the Antarctic region, except for localized areas along the sea-ice edge where model disagreement is more pronounced, particularly in the ABS and the Eastern Antarctic, and the coastal edges of the Weddell Sea along the Antarctic Peninsula (Fig.7a). When comparing across all the sea-ice products, a relatively

https://doi.org/10.5194/egusphere-2024-2744
Preprint. Discussion started: 3 April 2025

higher standard deviation value is noticed in most of the Antarctic regions with respect to the satellite product (Fig.7a). This can be attributed to the satellite product's exaggerated SIT values for September which most models are unable to simulate, leading to greater model disagreements.

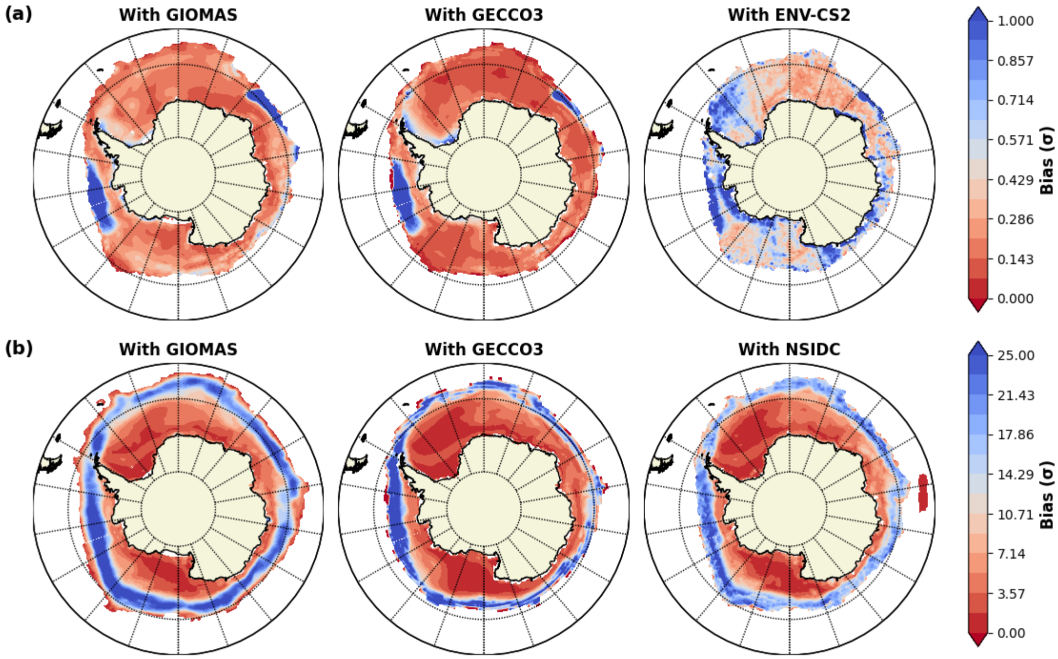

Figure 7: Variability of the Spatial Biases in CMIP6 Models (calculated as Standard Deviation of the difference between CMIP6 MMM and the three distinct sea ice products); for the month of September in (a) SIT (m) and (b) SIC (%).

Figure 7b shows SIC bias spreads for September, where much of the Antarctic region displays low standard deviation values. However, the sea-ice edge remains an area of higher model disagreement, similar to the SIT patterns, suggesting that while the ice interior is well-represented, models continue to struggle with accurately locating the ice edge. The correlation between SIC and SIT bias spreads is again observed in September, where model disagreements along localized ice edges occur in both variables, indicating that SIT biases in CMIP6 models may stem, in part, from uncertainties in where the ice edge is located. However, along the coastal edges of the Antarctic Peninsula, the lower SIC standard deviation values compared to that of SIT suggest that the model disagreements in SIT are more likely driven by the differences in how models simulate dynamic processes (e.g., the Weddell gyre and its role in sea-ice dynamics) rather than by inaccuracies in the ice edge representation. The following section addresses this in more detail across individual models.

3.4 Spatial Distributions of SIT

In this section, we perform a spatial comparison for circum-Antarctic SIT across 39 individual CMIP6 model ensembles using GIOMAS as the observational reference. Here, a reanalysis dataset

https://doi.org/10.5194/egusphere-2024-2744
Preprint. Discussion started: 3 April 2025

is selected as the reference instead of satellite products primarily due to the very high thickness biases observed in the latter during September (Fig.S1), and the closer alignment of models with the synthesis products in September (See Sec.3.1; Fig.1c). In general, during both the months the mean spatial distribution of SIT in the satellite product as well as GIOMAS show that thickest sea-ice resides in the western Weddell Sea along the Antarctic Peninsula and along the coastal edges of the ABS - in the form of multi-year ice (Fig.8 and S2). There is relatively thinner sea-ice observed in the eastern Antarctic (Kurtz & Markus, 2012). Our analysis reveals that most of the CMIP6 models capture a similar spatial pattern in SIT around the Antarctic however, they do exhibit biases and underestimate thickness (Fig.5 and Fig.S1-S3).

In February, over half of the models simulate thinner sea ice in the Weddell Sea compared to the reanalysis product (Fig.S2) while thin biases relative to the satellite products are simulated almost across all the models (Fig.S3). On the circum-Antarctica scale, about 38% of the models simulate thicker ice compared to GIOMAS, with only 5 out of 39 models showing thickness greater than that estimated by satellite products.

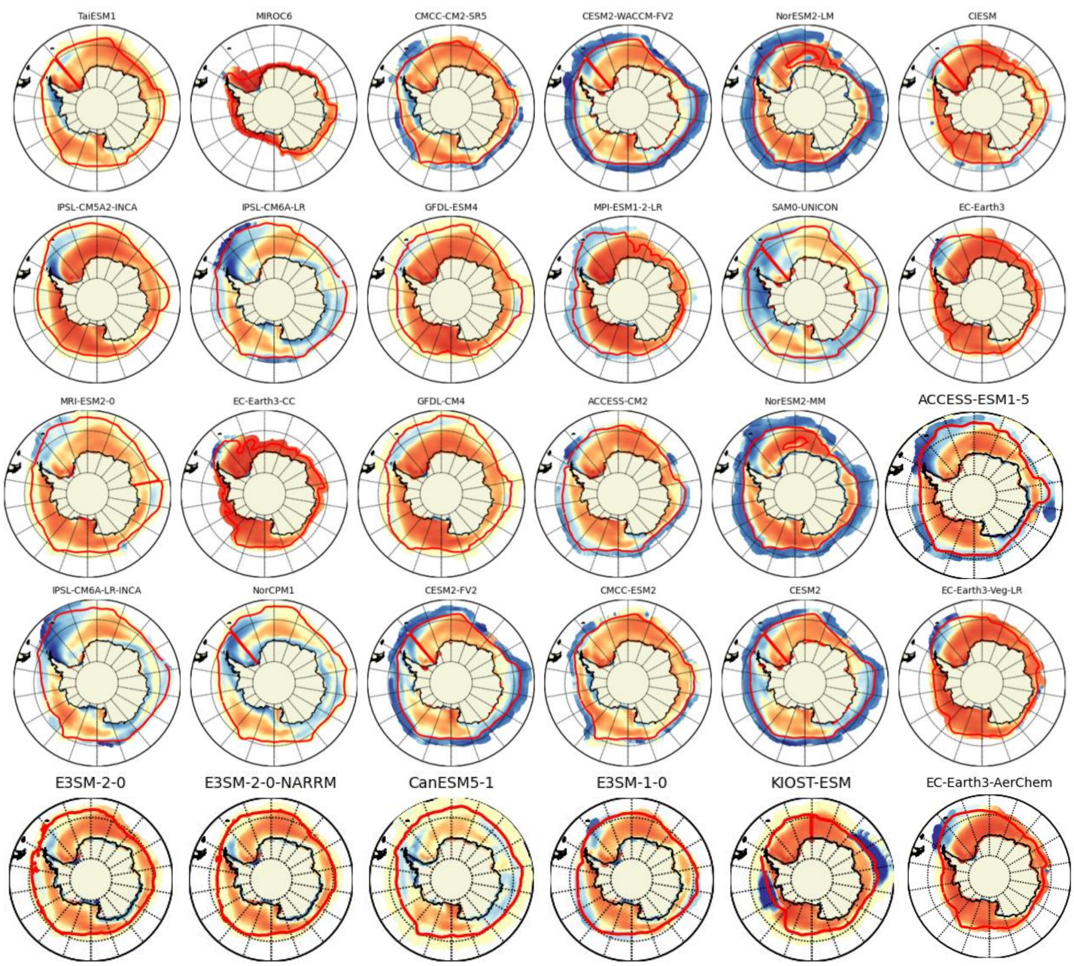

https://doi.org/10.5194/egusphere-2024-2744
Preprint. Discussion started: 3 April 2025

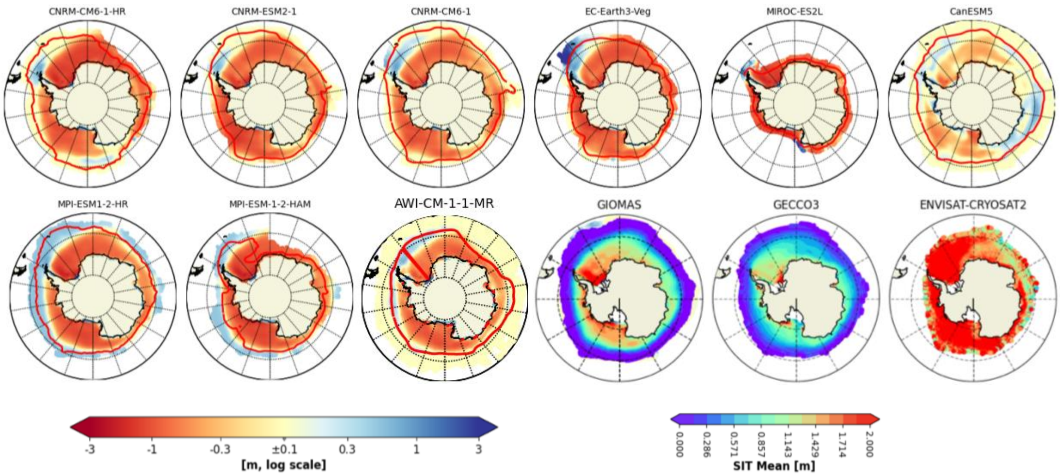

Figure 8: Spatial Biases of SIT averaged over 2002 to 2014 (September) for 39 CMIP6 models from the reference dataset: GIOMAS. The last three plots show the time averaged SIT for the three sea-ice products. The red contours represent the sea-ice edge.

The spatial patterns of SIT in September (Fig.8) show anomalously thick ice (>3m) in some CMIP6 models primarily in *two* regions: an elongated *tongue of thickest sea-ice* extending northward from the northwest Weddell Sea along the Antarctic Peninsula and, the other is *around the sea-ice edge*. The distinctive tongue-like pattern may be attributed to a prominent feature in the Weddell Sea called the *Weddell Gyre* (Vernet et al., 2019). This mechanism contributes significantly to the regional sea-ice dynamics in the form of an apparent westward ice motion in the southern Weddell Sea. As a result, ice convergence occurs in the southwestern Weddell, causing dynamic thickening (Shi et al., 2021). Multiple models, including IPSL-CM6A-, EC-Earth3-, NorCPM1, and ACCESS-models, which captured this tongue of thick sea-ice, also effectively captured the Weddell Gyre through their well-developed sea-ice velocity vectors (not shown). This is one of the primary reasons why these models simulate excessively thick ice along the Peninsula (Li et al., 2021). A similar spatial pattern in SIT was also observed using ICESat measurements (Holland & Kwok, 2012) and in simulations from an ocean-sea-ice model in the Southern Ocean (Holland et al., 2014).

The other region of thick sea-ice bias is the *sea-ice edge* (Fig.8). It's interesting to note that the CMIP6 models that have exhibited better performance in simulating Antarctic SIA, such as CESM2-, NorESM2-, and ACCESS-models (Holmes et al., 2019; Li et al., 2023; Roach et al., 2020; Uotila et al., 2014) show positive thickness anomalies/biases all around the sea-ice edge during September, north the 15% sea-ice concentration interval. A potential explanation for this could be through combinations of changes in air-ice drag and the direction of cold or warm-air advection. These may result in northward wind stress causing the sea-ice to drift, transport and accumulate causing dynamic convergence at the sea-ice edge (Singh et al., 2021; Holland et al., 2014; Holland & Kwok, 2012). Another reason could be the high-intensity ocean-wave fields linked to the Southern Ocean which deeply infiltrate the marginal ice zone. This penetration induces alterations in thickness distribution through processes like rafting and ridging, especially in the vicinity of the ice edge (Langhorne et al., 1998). In any case, the simulated sea-ice at the ice edge is much thicker than observed and further study is required to eliminate modeling error as its cause.

Among the CMIP6 models, there are two clear patterns that emerge across the smaller subsets (Fig.8): *First*, a general "thin" bias in the models which is observed throughout the ice pack at all longitudes, coupled with a "thick" bias in the marginal ice zone/ice edge (as seen in CESM2, NorESM2, and ACCESS), likely reflecting the net northward transport of Antarctic sea-ice. *Second*, another smaller subset of models (such as IPSL, SAM0-UNICON, NorCPM1, CESM2, and CanESM5) which exhibit more zonally assymmetric biases, providing distinct signatures of the Ross and Weddell gyres—particularly in the form of thick ice at the outflow and thin ice at the inflow. Both modeled patterns underscore the importance of sea-ice dynamics and invites further investigation.

Additionally, Fig.8 and S1-S5 depict varying model spreads in SIT simulations with noticeable differences in their spatial biases and distributions. These variations are largely driven by differences in parameterization schemes and the representation of underlying physical processes across the models. While these discrepancies affect the accuracy of SIT simulations, a detailed examination of each model's parameterization and physics is beyond the scope of this study. Our primary focus is on the broader evaluation of the spatial distribution of SIT across the models and their comparison to observational and synthesis datasets.

In summary, all models tend to underestimate SIT and produce relatively thinner sea-ice during both September and February. These negative biases are more pronounced in September and much less pronounced in February. When comparing among the reference products, models simulate SIT closer to the reanalysis reference, i.e. GIOMAS, in both months with about 50% of the CMIP6 models (20 out of 39) having their mean spatial biases between +/-0.5m. Notably, one of our comparisons uses satellite products, which exhibit some uncertainties in estimating SIT in the Southern Ocean, particularly showing thicker values in September. Therefore, models displaying even greater positive biases (>1m) in September compared to the satellites (Fig.S1) may be simulating excessively thick sea-ice, potentially presenting a false picture of future Antarctic sea-ice changes.

4. Discussion and Conclusions

Given the current context of recent extreme sea-ice loss, it is imperative to develop predictions regarding Antarctic sea-ice behavior to enhance our understanding of its future variability and response to climate change. For this we need reliable SIT estimates along with the surface sea-ice variables, to assess the absolute changes in the global sea-ice cover. However, due to the lack of long-term, high-quality observation datasets, assessing Antarctic SIT and its climatic response remains challenging.

While GCMs offer a valuable solution to the above challenge, there is an understanding that they do not yet accurately simulate SIT and SIV. However, it is still necessary to see how well they perform even if only to understand where more work is needed. Therefore, despite existing limitations, this study undertook a comprehensive evaluation of Antarctic SIT and SIV by comparing 39 CMIP6 model outputs with three different sea-ice products. This comparison demonstrates that models can provide longer timescales of SIT data, which, when compared with

https://doi.org/10.5194/egusphere-2024-2744
Preprint. Discussion started: 3 April 2025

observations-based sea-ice estimates (and accounting for their limitations), can enhance our understanding of Antarctic sea-ice.

An accurate modeling of climatological mean sea-ice cover in the GCMs is an initial step and a necessary condition for accurate projections (Holmes et al., 2022). In line with this, our study shows that most CMIP6 models can simulate the timing of annual cycles of all the sea-ice variables much like the sea-ice products. For SIT, the greatest agreement is observed during the maximum in February, when the Southern Ocean retains the thickest sea-ice, consisting of very thick ice that survives the summer. However, models fail to capture the SIT minima as observed in the satellite products and instead align more closely with the synthesis estimates (GIOMAS and GECCO3), with the minima of both models and synthesis estimates occurring in May. For SIV, the CMIP6 MMM-based annual maxima are lagged by 1 and 2 months compared to the satellite products and GIOMAS, respectively. The closest agreement in the annual cycles between models and sea-ice products is seen in SIA. Despite this alignment, when examined numerically, the models substantially underestimate the annual cycles across all the variables, with relatively lower biases occurring in SIA. Biases in the modeled cycles of SIV and SIA are higher in April-October, with greater inter-model spreads in fall-winter. Conversely, SIT inter-model spreads are higher during November-March but exhibit relatively lower biases compared to the satellite dataset.

CMIP6 models continue to simulate negative trends in Antarctic SIT/SIV, contrary to the observed positive trends, until mid-2015. Additionally, we observe positive trends in SIT/SIV during the cooler seasons, which are absent in SIA. These positive trends may be due to intensified seasonal winds during the cooler seasons and further imply that the variability in total sea-ice mass in these months could be influenced by thickness/volume changes. We also examined seasonal variations in sea-ice correlations, showing positive (negative) relationships between SIA and SIT during September (February). Such seasonal covariances suggest that surface sea-ice parameters such as SIA may be weak predictors of SIT. This in turn can have significant implications for our understanding of absolute sea-ice changes in the Antarctic when based solely on SIA. Investigating the reasons for such covariances is outside the scope of this study.

This study compares the SIT biases using the multi-model means, where we show that model results are closer to the reanalysis/synthesis datasets both over both space and time. The spatial variability of sea-ice biases in CMIP6 models highlights certain challenges in accurately capturing both SIT and SIC, especially near the ice edges. Models exhibit greater disagreement in regions influenced by dynamic processes like ice advection, melting, and freezing, while better agreement is seen in areas with multi-year sea-ice and inner ice packs. The variability in SIT biases is found to be closely linked to uncertainties in the model representation of the ice edge, suggesting that improvements in capturing both the dynamic processes and the correct ice edge location could enhance model performance in simulating sea-ice cover in these areas.

While many CMIP6 models simulate spatial SIT patterns similar to the three sea-ice products, they generally tend to underestimate SIT, especially during September. Intriguingly, certain models display anomalously thick sea-ice along the Peninsula and around the sea-ice edges, even greater than the reference dataset. A potential explanation for the observed thick ice in the Weddell can be the presence of fast-ice (i.e., sea-ice pinned to the coast or grounded icebergs). Such thicknesses observed around the Antarctic Peninsula in Fig.8 significantly exceed what is expected from atmospheric heat loss alone, suggesting the presence of fast ice (Fraser et al., 2023). However, we note that the GCMs do not simulate such landfast ice prognostically. Hence, accumulation of thick

https://doi.org/10.5194/egusphere-2024-2744
Preprint. Discussion started: 3 April 2025

ice in this region, as depicted in the models, is likely driven by dynamic processes such as winds or drift, leading to ice piling up against the Antarctic Peninsula.

The presence of such model deviations can hamper our understanding of climate-sea-ice interactions as well as biological feedback between the oceans and climate. For instance, due to the existing relationships between SIT and sea-ice motion, biases in the simulated thickness will also affect the dynamics in the models which in turn will impact our understanding of the overall Antarctic sea-ice trends in the models (Lecomte et al., 2016; Sun and Eisenman, 2021). Additionally, lower SIT could create the misleading impression of lower albedo and increased light penetration, subsequently leading to increased Primary Production (Jeffery et al., 2020). Our study does not explore the reasons behind such continued biases in CMIP6. However, their potential explanations may include cloud effects (Kay et al., 2016; Zelinka et al., 2020), spatial resolution that does not permit eddies, which are understood to be highly important for representation of Southern Ocean dynamics (Poulsen et al., 2018; Rackow et al., 2019), models lacking grounded icebergs as landfast ice (Fraser et al., 2023), biases in Southern Ocean stratification (Martinson and Iannuzzi, 1998), and temperature (Luo et al., 2023) and, the lack of coupled ice sheet interactions, which have relevance for the entire Antarctic climate system (Bronselaer et al., 2018; Golledge et al., 2019; Purich & England, 2023).

Considering the above findings, we anticipate that future studies will investigate these aspects with respect to Antarctic SIT. Addressing such model biases could be initial steps in further improving the representation of dynamic processes in sea-ice, climate, and biogeochemical models, ensuring their accurate predictions. Understanding the biases in sea-ice parameters and physical mechanisms behind these constraints will lead to improvement in the reliability of sea-ice projections and increase confidence in our understanding of what controls the rate of Antarctic sea-ice loss. Therefore, our research addresses a critical knowledge gap of understanding and modeling of Antarctic SIT and the dynamics involved in shaping its temporal and spatial distributions using the long-term coupled climate simulations.

Author contributions

ST and MR developed the concept of the paper. ST analyzed all the data and wrote the first draft of the paper. WH helped with the methodology and analysis of the CMIP6 modeled data. All authors assisted during the writing process and critically discussed the contents.

Competing interests

The authors declare that they have no conflict of interest.

Data Availability Statement

The satellite products used in the study are available at https://catalogue.ceda.ac.uk/uuid/b1f1ac03077b4aa784c5a413a2210bf5 for Envisat and at https://catalogue.ceda.ac.uk/uuid/48fc3d1e8ada405c8486ada522dae9e8 for CryoSat-2 (Hendricks et al., 2018a, 2018b). The GECCO3 sea-ice thickness data are available at https://www.cen.uni-hamburg.de/icdc/data/ocean/easy-init-ocean/gecco3.html last access: 31 May 2021, Köhl, 2020). The GIOMAS sea-ice thickness data are available at https://psc.apl.washington.edu/zhang/Global_seaice/data.html (last access:26 December 2020, Zhang and Rothrick, 2003). Monthly values of sea-ice concentration from NSIDC are available at https://nsidc.org/data/nsidc-0079/versions/3. All the CMIP6 model datasets are available at ESGF website: https://aims2.llnl.gov/search/cmip6/ (Table S2).

Acknowledgement

M.R. Raphael and S. Trivedi acknowledge funding by the National Science Foundation (NSF) under the Office of Polar Programs (NSF-OPP-1745089). W.R. Hobbs acknowledges support by the Australian Government as part of the Antarctic Science Collaboration Initiative program and receives funding from the Australian Research Council Discovery Project (DP230102994).

References

Abernathey, R.P., Cerovecki, I., Holland, P.R., Newsom, E., Mazloff, M. and Talley, L.D.: Water-mass transformation by sea ice in the upper branch of the Southern Ocean overturning. *Nature Geoscience*, *9*(8), pp.596-601, 2016.

Behrendt, A., Dierking, W., Fahrbach, E., & Witte, H. (2013). Sea ice draft in the Weddell Sea, measured by upward looking sonars. *Earth System Science Data*, *5*(1), 209–226. https://doi.org/10.5194/essd-5-209-2013

Bronselaer, B., Winton, M., Griffies, S. M., Hurlin, W. J., Rodgers, K. B., Sergienko, O. V., Stouffer, R. J., & Russell, J. L. (2018). Change in future climate due to Antarctic meltwater. *Nature*, *564*(7734), Article 7734. https://doi.org/10.1038/s41586-018-0712-z

Cavalieri, D. J., & Parkinson, C. L. (2008). Antarctic sea ice variability and trends, 1979–2006. *Journal of Geophysical Research: Oceans*, *113*(C7). https://doi.org/10.1029/2007JC004564

Comiso, J. C. (2017). Bootstrap Sea Ice Concentrations from Nimbus-7 SMMR and DMSP SSM/I-SSMIS, Version 3 [Data Set]. Boulder, Colorado USA. NASA National Snow and Ice Data Center Distributed Active Archive Center. https://doi.org/10.5067/7Q8HCCWS4I0R. Date Accessed 04-30-2024.

Döscher, R., Acosta, M., Alessandri, A., Anthoni, P., Arsouze, T., Bergman, T., ... & Zhang, Q. (2022). The EC-Earth3 Earth system model for the coupled model intercomparison project 6. *Geosci Model Dev 15 (7): 2973–3020.*

Eayrs, C., Holland, D., Francis, D., Wagner, T., Kumar, R., & Li, X. (2019). Understanding the Seasonal Cycle of Antarctic Sea Ice Extent in the Context of Longer-Term Variability. *Reviews of Geophysics*, *57*(3), 1037–1064. https://doi.org/10.1029/2018RG000631

Eayrs, C., Li, X., Raphael, M. N., & Holland, D. M. (2021). Rapid decline in Antarctic sea ice in recent years hints at future change. *Nature Geoscience*, *14*(7), 460–464. https://doi.org/10.1038/s41561-021-00768-3

Eyring, V., Gleckler, P. J., Heinze, C., Stouffer, R. J., Taylor, K. E., Balaji, V., Guilyardi, E., Joussaume, S., Kindermann, S., Lawrence, B. N., Meehl, G. A., Righi, M., & Williams, D. N. (2016). Towards improved and more routine Earth system model evaluation in CMIP. *Earth System Dynamics*, *7*(4), 813–830. https://doi.org/10.5194/esd-7-813-2016

Fraser, A. D., Wongpan, P., Langhorne, P. J., Klekociuk, A. R., Kusahara, K., Lannuzel, D., Massom, R. A., Meiners, K. M., Swadling, K. M., Atwater, D. P., Brett, G. M., Corkill,

https://doi.org/10.5194/egusphere-2024-2744
Preprint. Discussion started: 3 April 2025

M., Dalman, L. A., Fiddes, S., Granata, A., Guglielmo, L., Heil, P., Leonard, G. H., Mahoney, A. R., … Wienecke, B. (2023). Antarctic Landfast Sea Ice: A Review of Its Physics, Biogeochemistry and Ecology. *Reviews of Geophysics*, *61*(2), e2022RG000770. https://doi.org/10.1029/2022RG000770

Golledge, N. R., Keller, E. D., Gomez, N., Naughten, K. A., Bernales, J., Trusel, L. D., & Edwards, T. L. (2019). Global environmental consequences of twenty-first-century ice-sheet melt. *Nature*, *566*(7742), Article 7742. https://doi.org/10.1038/s41586-019-0889-9

Haumann, F. A., Gruber, N., Münnich, M., Frenger, I., & Kern, S. (2016). Sea-ice transport driving Southern Ocean salinity and its recent trends. *Nature*, *537*(7618), 89–92. https://doi.org/10.1038/nature19101

Hendricks S, Paul S and Rinne E (2018a): ESA sea ice climate change initiative (sea_ice_cci): Southern hemisphere sea ice thickness from the CryoSat-2 satellite on a monthly grid (L3C), v2.0 (https://doi.org/10.5285/48fc3d1e8ada405c8486ada522dae9e8)

Hendricks S, Paul S and Rinne E (2018b): ESA sea ice climate change initiative (Sea_Ice_cci): Southern hemisphere sea ice thickness from the Envisat satellite on a monthly grid(L3C), v2.0 (https://doi.org/10.5285/b1f1ac03077b4aa784c5a413a2210bf5)

Hobbs, W., Massom, R., Stammerjohn, S., Reid, P., Williams, G., & Meier, W. (2016). A review of recent changes in Southern Ocean sea ice, their drivers and forcings. *Global and Planetary Change*, *143*. https://doi.org/10.1016/j.gloplacha.2016.06.008

Holland, M. M., Bitz, C. M., Hunke, E. C., Lipscomb, W. H., & Schramm, J. L. (2006). Influence of the Sea Ice Thickness Distribution on Polar Climate in CCSM3. *Journal of Climate*, *19*(11), 2398–2414. https://doi.org/10.1175/JCLI3751.1

Holland, P. R., Bruneau, N., Enright, C., Losch, M., Kurtz, N. T., & Kwok, R. (2014). Modeled trends in Antarctic sea ice thickness. *Journal of Climate*, *27*(10), 3784-3801.

Holland, P. R., & Kwok, R. (2012). Wind-driven trends in Antarctic sea-ice drift. *Nature Geoscience*, *5*(12), 872–875. https://doi.org/10.1038/ngeo1627

Holmes, C. R., Bracegirdle, T. J., & Holland, P. R. (2022). Antarctic Sea Ice Projections Constrained by Historical Ice Cover and Future Global Temperature Change. *Geophysical Research Letters*, *49*(10), e2021GL097413. https://doi.org/10.1029/2021GL097413

Holmes, C. R., Holland, P. R., & Bracegirdle, T. J. (2019). Compensating Biases and a Noteworthy Success in the CMIP5 Representation of Antarctic Sea Ice Processes. *Geophysical Research Letters*, *46*(8), 4299–4307. https://doi.org/10.1029/2018GL081796

Hou, Y., Nie, Y., Min, C., Shu, Q., Luo, H., Liu, J., & Yang, Q. (2024). Evaluation of Antarctic sea ice thickness and volume during 2003–2014 in CMIP6 using Envisat and CryoSat-2 observations. *Environmental Research Letters*, 19(1), 014067.

Jeffery, N., Maltrud, M. E., Hunke, E. C., Wang, S., Wolfe, J., Turner, A. K., Burrows, S. M., Shi, X., Lipscomb, W. H., Maslowski, W., & Calvin, K. V. (2020). Investigating controls on sea ice algal production using E3SMv1.1-BGC. *Annals of Glaciology*, *61*(82), 51–72. https://doi.org/10.1017/aog.2020.7

Kacimi, S., & Kwok, R. (2020). The Antarctic sea ice cover from ICESat-2 and CryoSat-2: freeboard, snow depth, and ice thickness. *The Cryosphere*, 14(12), 4453-4474.

Kay, J. E., Wall, C., Yettella, V., Medeiros, B., Hannay, C., Caldwell, P., & Bitz, C. (2016). Global Climate Impacts of Fixing the Southern Ocean Shortwave Radiation Bias in the Community Earth System Model (CESM). *Journal of Climate*, *29*(12), 4617–4636. https://doi.org/10.1175/JCLI-D-15-0358.1

https://doi.org/10.5194/egusphere-2024-2744
Preprint. Discussion started: 3 April 2025

Koenig, L., Martin, S., Studinger, M., & Sonntag, J. (2010). Polar Airborne Observations Fill Gap in Satellite Data. *Eos, Transactions American Geophysical Union*, *91*(38), 333–334. https://doi.org/10.1029/2010EO380002

Köhl, A. (2020). Evaluating the GECCO3 1948–2018 ocean synthesis – a configuration for initializing the MPI-ESM climate model. *Quarterly Journal of the Royal Meteorological Society*, *146*(730), 2250–2273. https://doi.org/10.1002/qj.3790

Kumar, A., Dwivedi, S., & Rajak, D. R. (2017). Ocean sea-ice modelling in the Southern Ocean around Indian Antarctic stations. *Journal of Earth System Science*, *126*(5), 70. https://doi.org/10.1007/s12040-017-0848-5

Kurtz, N. T., & Markus, T. (2012). Satellite observations of Antarctic sea ice thickness and volume. *Journal of Geophysical Research: Oceans*, *117*(C8). https://doi.org/10.1029/2012JC008141

Kusahara, K., Hasumi, H., Fraser, A. D., Aoki, S., Shimada, K., Williams, G. D., Massom, R., & Tamura, T. (2017). Modeling Ocean–Cryosphere Interactions off Adélie and George V Land, East Antarctica. *Journal of Climate*, *30*(1), 163–188. https://doi.org/10.1175/JCLI-D-15-0808.1

Langhorne, P. J., Squire, V. A., Fox, C., & Haskell, T. G. (1998). Break-up of sea ice by ocean waves. *Annals of Glaciology*, *27*, 438–442. https://doi.org/10.3189/S0260305500017869

Lecomte, O., Goosse, H., Fichefet, T., Holland, P. R., Uotila, P., Zunz, V., & Kimura, N. (2016). Impact of surface wind biases on the Antarctic sea ice concentration budget in climate models. *Ocean Modelling*, 105, 60-70.

Li, S., Zhang, Y., Chen, C., Zhang, Y., Xu, D., & Hu, S. (2023). Assessment of Antarctic Sea Ice Cover in CMIP6 Prediction with Comparison to AMSR2 during 2015–2021. *Remote Sensing*, *15*(8), 2048. https://doi.org/10.3390/rs15082048

Li, S., Huang, G., Li, X., Liu, J., & Fan, G. (2021). An assessment of the Antarctic sea ice mass budget simulation in CMIP6 historical experiment. *Frontiers in Earth Science*, *9*, 649743.

Liao, S., Luo, H., Wang, J., Shi, Q., Zhang, J., & Yang, Q. (2022). An evaluation of Antarctic sea-ice thickness from the Global Ice-Ocean Modeling and Assimilation System based on in situ and satellite observations. *The Cryosphere*, *16*(5), 1807–1819. https://doi.org/10.5194/tc-16-1807-2022

Lindsay, R. W., & Zhang, J. (2006). Assimilation of Ice Concentration in an Ice–Ocean Model. *Journal of Atmospheric and Oceanic Technology*, *23*(5), 742–749. https://doi.org/10.1175/JTECH1871.1

Luo, F., Ying, J., Liu, T., & Chen, D.: Origins of Southern Ocean warm sea surface temperature bias in CMIP6 models. *npj Climate and Atmospheric Science, 6(1), 127,* 2023.

Maksym, T., Stammerjohn, S., Ackley, S., & Massom, R. (2012). Antarctic Sea Ice—A Polar Opposite? *Oceanography*, 25(3),140–151. https://doi.org/10.5670/oceanog.2012.88

Martinson, D. G., & Iannuzzi, R. A.: Antarctic ocean-ice interaction: Implications from ocean bulk property distributions in the Weddell Gyre. *Antarctic sea ice: physical processes, interactions and variability*, *74*, 243-271, 1998.

Martinson, D. G. (2012). Antarctic circumpolar current's role in the Antarctic ice system: An overview. *Palaeogeography, Palaeoclimatology, Palaeoecology*, *335*, 71-74.

Massom, R. A., & Stammerjohn, S. E. (2010). Antarctic sea ice change and variability – Physical and ecological implications. *Polar Science*, *4*(2), 149–186. https://doi.org/10.1016/j.polar.2010.05.001

Massonnet, F., Mathiot, P., Fichefet, T., Goosse, H., König Beatty, C., Vancoppenolle, M., & Lavergne, T. (2013). A model reconstruction of the Antarctic sea ice thickness and volume changes over 1980–2008 using data assimilation. *Ocean Modelling*, *64*, 67–75. https://doi.org/10.1016/j.ocemod.2013.01.003

Meredith, M., Sommerkorn, M., Cassotta, S., Derksen, C., Ekaykin, A., Hollowed, A., ... & Schuur, E. A. G. (2019). Polar regions. chapter 3, ipcc special report on the ocean and cryosphere in a changing climate.

Notz, D., & Community, S. (2020). Arctic Sea Ice in CMIP6. *Geophysical Research Letters*, *47*(10), e2019GL086749. https://doi.org/10.1029/2019GL086749

Parkinson, C. L., & Cavalieri, D. J. (2012). Antarctic sea ice variability and trends, 1979–2010. *The Cryosphere*, *6*(4), 871–880. https://doi.org/10.5194/tc-6-871-2012

Paul, S., Hendricks, S., Ricker, R., Kern, S., & Rinne, E. (2018). Empirical parametrization of Envisat freeboard retrieval of Arctic and Antarctic sea ice based on CryoSat-2: Progress in the ESA Climate Change Initiative. *The Cryosphere*, *12*. https://doi.org/10.5194/tc-12-2437-2018

Pellichero, V., Sallée, J.-B., Chapman, C. C., & Downes, S. M. (2018). The southern ocean meridional overturning in the sea-ice sector is driven by freshwater fluxes. *Nature Communications*, *9*(1), 1789. https://doi.org/10.1038/s41467-018-04101-2

Poulsen, M. B., Jochum, M., & Nuterman, R. (2018). Parameterized and resolved Southern Ocean eddy compensation. *Ocean Modelling*, *124*, 1–15. https://doi.org/10.1016/j.ocemod.2018.01.008

Purich, A., & England, M. H. (2023). Projected Impacts of Antarctic Meltwater Anomalies over the Twenty-First Century. *Journal of Climate*, *36*(8), 2703–2719. https://doi.org/10.1175/JCLI-D-22-0457.1

Rackow, T., Sein, D. V., Semmler, T., Danilov, S., Koldunov, N. V., Sidorenko, D., Wang, Q., & Jung, T. (2019). Sensitivity of deep ocean biases to horizontal resolution in prototype CMIP6 simulations with AWI-CM1.0. *Geoscientific Model Development*, *12*(7), 2635–2656. https://doi.org/10.5194/gmd-12-2635-2019

Roach, L. A., Dörr, J., Holmes, C. R., Massonnet, F., Blockley, E. W., Notz, D., Rackow, T., Raphael, M. N., O'Farrell, S. P., Bailey, D. A., & Bitz, C. M. (2020). Antarctic Sea Ice Area in CMIP6. *Geophysical Research Letters*, *47*(9), e2019GL086729. https://doi.org/10.1029/2019GL086729

Sallée, J. B., Abrahamsen, E. P., Allaigre, C., Auger, M., Ayres, H., Badhe, R., Boutin, J., Brearley, J. A., de Lavergne, C., ten Doeschate, A. M. M., Droste, E. S., du Plessis, M. D., Ferreira, D., Giddy, I. S., Gülk, B., Gruber, N., Hague, M., Hoppema, M., Josey, S. A., … Zhou, S. (n.d.). Southern ocean carbon and heat impact on climate. *Philosophical Transactions. Series A, Mathematical, Physical, and Engineering Sciences*, *381*(2249), 20220056. https://doi.org/10.1098/rsta.2022.0056

Schultz, C. (2013). Antarctic sea ice thickness affects algae populations. *Eos, Transactions American Geophysical Union*, *94*. https://doi.org/10.1002/2013EO030032

Schwegmann, S., Rinne, E., Ricker, R., Hendricks, S., & Helm, V. (2016). About the consistency between Envisat and CryoSat-2 radar freeboard retrieval over Antarctic sea ice. *The Cryosphere*, *10*(4), 1415–1425. https://doi.org/10.5194/tc-10-1415-2016

Shi, Q., Yang, Q., Mu, L., Wang, J., Massonnet, F., & Mazloff, M. R. (2021). Evaluation of sea-ice thickness from four reanalyses in the Antarctic Weddell Sea. *The Cryosphere*, *15*(1), 31–47. https://doi.org/10.5194/tc-15-31-2021

https://doi.org/10.5194/egusphere-2024-2744
Preprint. Discussion started: 3 April 2025

Shu, Q., Song, Z., & Qiao, F. (2015). Assessment of sea ice simulations in the CMIP5 models. *The Cryosphere*, *9*(1), 399–409. https://doi.org/10.5194/tc-9-399-2015

Shu, Q., Wang, Q., Song, Z., Qiao, F., Zhao, J., Chu, M., & Li, X. (2020). Assessment of Sea Ice Extent in CMIP6 With Comparison to Observations and CMIP5. *Geophysical Research Letters*, *47*(9), e2020GL087965. https://doi.org/10.1029/2020GL087965

Singh, H. K. A., Landrum, L., Holland, M. M., Bailey, D. A., & DuVivier, A. K. (2021). An Overview of Antarctic Sea Ice in the Community Earth System Model Version 2, Part I: Analysis of the Seasonal Cycle in the Context of Sea Ice Thermodynamics and Coupled Atmosphere-Ocean-Ice Processes. *Journal of Advances in Modeling Earth Systems*, *13*(3), e2020MS002143. https://doi.org/10.1029/2020MS002143

Stammerjohn, S., Martinson, D., Smith, R., Yuan, X., & Rind, D. (2008). Trends in Antarctic annual sea ice retreat and advance and their relation to El Niño-Southern Oscillation and Southern Annular Mode variability. *Journal of Geophysical Research: Oceans*, *113*.

St-Laurent, P., Yager, P. L., Sherrell, R. M., Stammerjohn, S. E., & Dinniman, M. S. (2017). Pathways and supply of dissolved iron in the Amundsen Sea (Antarctica). *Journal of Geophysical Research: Oceans*, *122*(9), 7135–7162. https://doi.org/10.1002/2017JC013162

Stroeve, J., Barrett, A., Serreze, M., & Schweiger, A. (2014). Using records from submarine, aircraft and satellites to evaluate climate model simulations of Arctic sea ice thickness. *The Cryosphere*, *8*(5), 1839–1854. https://doi.org/10.5194/tc-8-1839-2014

Sun, S., & Eisenman, I. (2021). Observed Antarctic sea ice expansion reproduced in a climate model after correcting biases in sea ice drift velocity. *Nature communications*, 12(1), 1060.

Tilling, R., Ridout, A., & Shepherd, A. (2019). Assessing the Impact of Lead and Floe Sampling on Arctic Sea Ice Thickness Estimates from Envisat and CryoSat-2. *Journal of Geophysical Research: Oceans*, *124*(11), Article 11.

Turner, J., Bracegirdle, T. J., Phillips, T., Marshall, G. J., & Hosking, J. S. (2013). An Initial Assessment of Antarctic Sea Ice Extent in the CMIP5 Models. *Journal of Climate*, *26*(5), 1473–1484. https://doi.org/10.1175/JCLI-D-12-00068.1

Turner, J., Hosking, J. S., Bracegirdle, T. J., Marshall, G. J., & Phillips, T. (2015). Recent changes in Antarctic Sea Ice. *Philosophical Transactions of the Royal Society A: Mathematical, Physical and Engineering Sciences*, *373*(2045), 20140163. https://doi.org/10.1098/rsta.2014.0163

Uotila, P., Holland, P. R., Vihma, T., Marsland, S. J., & Kimura, N. (2014). Is realistic Antarctic sea-ice extent in climate models the result of excessive ice drift? *Ocean Modelling*, *79*, 33–42. https://doi.org/10.1016/j.ocemod.2014.04.004

Van Achter, G., Fichefet, T., Goosse, H., Pelletier, C., Sterlin, J., Huot, P.-V., Lemieux, J.-F., Fraser, A. D., Haubner, K., & Porter-Smith, R. (2022). Modelling landfast sea ice and its influence on ocean–ice interactions in the area of the Totten Glacier, East Antarctica. *Ocean Modelling*, *169*, 101920. https://doi.org/10.1016/j.ocemod.2021.101920

Vernet, M., Geibert, W., Hoppema, M., Brown, P. J., Haas, C., Hellmer, H. H., Jokat, W., Jullion, L., Mazloff, M., Bakker, D. C. E., Brearley, J. A., Croot, P., Hattermann, T., Hauck, J., Hillenbrand, C.-D., Hoppe, C. J. M., Huhn, O., Koch, B. P., Lechtenfeld, O. J., … Verdy, A. (2019). The Weddell Gyre, Southern Ocean: Present Knowledge and Future Challenges. *Reviews of Geophysics*, *57*(3), 623–708. https://doi.org/10.1029/2018RG000604

https://doi.org/10.5194/egusphere-2024-2744
Preprint. Discussion started: 3 April 2025

Voldoire, A., Saint-Martin, D., Sénési, S., Decharme, B., Alias, A., Chevallier, M., ... & Waldman, R.: Evaluation of CMIP6 deck experiments with CNRM-CM6-1. *Journal of Advances in Modeling Earth Systems*, *11*(7), 2177-2213, 2019.

Wang, J., Min, C., Ricker, R., Shi, Q., Han, B., Hendricks, S., Wu, R., & Yang, Q. (2022). A comparison between Envisat and ICESat sea ice thickness in the Southern Ocean. *The Cryosphere*, *16*(10), 4473–4490. https://doi.org/10.5194/tc-16-4473-2022

Willatt, R. C., Giles, K. A., Laxon, S. W., Stone-Drake, L., & Worby, A. P. (2010). Field Investigations of Ku-Band Radar Penetration Into Snow Cover on Antarctic Sea Ice. *IEEE Transactions on Geoscience and Remote Sensing*, *48*(1), 365–372. https://doi.org/10.1109/TGRS.2009.2028237

Williams, R. G., Ceppi, P., Roussenov, V., Katavouta, A., & Meijers, A. J. (2023). The role of the Southern Ocean in the global climate response to carbon emissions. *Philosophical Transactions of the Royal Society A, 381(2249),* 20220062.

Worby, A. P., Geiger, C. A., Paget, M. J., Woert, M. L. V., Ackley, S. F., & DeLiberty, T. L. (2008). Thickness distribution of Antarctic sea ice. *Journal of Geophysical Research: Oceans*, *113*(C5). https://doi.org/10.1029/2007JC004254

Xu, Y., Li, H., Liu, B., Xie, H., & Ozsoy-Cicek, B. (2021). Deriving Antarctic Sea-Ice Thickness From Satellite Altimetry and Estimating Consistency for NASA's ICESat/ICESat-2 Missions. *Geophysical Research Letters*, *48*(20), e2021GL093425. https://doi.org/10.1029/2021GL093425

Zelinka, M. D., Myers, T. A., McCoy, D. T., Po-Chedley, S., Caldwell, P. M., Ceppi, P., Klein, S. A., & Taylor, K. E. (2020). Causes of Higher Climate Sensitivity in CMIP6 Models. *Geophysical Research Letters*, *47*(1), e2019GL085782. https://doi.org/10.1029/2019GL085782

Zhang, J. (2014). Modeling the Impact of Wind Intensification on Antarctic Sea Ice Volume. *Journal of Climate*, *27*(1), 202–214. https://doi.org/10.1175/JCLI-D-12-00139.1

Zhang, J., & Rothrock, D. A. (2003). Modeling Global Sea Ice with a Thickness and Enthalpy Distribution Model in Generalized Curvilinear Coordinates. *Monthly Weather Review*, *131*(5), 845–861. https://doi.org/10.1175/1520-0493(2003)131<0845:MGSIWA>2.0.CO;2

Zwally, H. J., Comiso, J. C., Parkinson, C. L., Cavalieri, D. J., & Gloersen, P. (2002). Variability of Antarctic sea ice 1979–1998. *Journal of Geophysical Research: Oceans*, *107*(C5), 9-1-9–19. https://doi.org/10.1029/2000JC000733

References for Supporting Material:

Bader, David C.; Leung, Ruby; Taylor, Mark; McCoy, Renata B. (2019). *E3SM-Project E3SM1.0 model output prepared for CMIP6 CMIP*. Version *YYYYMMDD*[1].Earth System Grid Federation. https://doi.org/10.22033/ESGF/CMIP6.2294

Cherchi, A., Fogli, P. G., Lovato, T., Peano, D., Iovino, D., Gualdi, S., Masina, S., Scoccimarro, E., Materia, S., Bellucci, A., & Navarra, A. (2019). Global Mean Climate and Main

https://doi.org/10.5194/egusphere-2024-2744
Preprint. Discussion started: 3 April 2025

Patterns of Variability in the CMCC-CM2 Coupled Model. Journal of Advances in Modeling Earth Systems, 11(1), 185–209. https://doi.org/10.1029/2018MS001369

Counillon, F., Keenlyside, N., Bethke, I., Wang, Y., Billeau, S., Shen, M.-L., & Bentsen, M. (2016). Flow-dependent assimilation of sea surface temperature in isopycnal coordinates with the Norwegian Climate Prediction Model. Tellus A, 68. https://doi.org/10.3402/tellusa.v68.32437

Danabasoglu, G., Lamarque, J.-F., Bacmeister, J., Bailey, D. A., DuVivier, A. K., Edwards, J., Emmons, L. K., Fasullo, J., Garcia, R., Gettelman, A., Hannay, C., Holland, M. M., Large, W. G., Lauritzen, P. H., Lawrence, D. M., Lenaerts, J. T. M., Lindsay, K., Lipscomb, W. H., Mills, M. J., … Strand, W. G. (2020). The Community Earth System Model Version 2 (CESM2). Journal of Advances in Modeling Earth Systems, 12(2), e2019MS001916. https://doi.org/10.1029/2019MS001916

Döscher, R., Acosta, M., Alessandri, A., Anthoni, P., Arsouze, T., Bergman, T., Bernardello, R., Boussetta, S., Caron, L.-P., Carver, G., Castrillo, M., Catalano, F., Cvijanovic, I., Davini, P., Dekker, E., Doblas-Reyes, F. J., Docquier, D., Echevarria, P., Fladrich, U., … Zhang, Q. (2022). The EC-Earth3 Earth system model for the Coupled Model Intercomparison Project 6. Geoscientific Model Development, 15(7), 2973–3020. https://doi.org/10.5194/gmd-15-2973-2022

Gettelman, A., Mills, M. J., Kinnison, D. E., Garcia, R. R., Smith, A. K., Marsh, D. R., Tilmes, S., Vitt, F., Bardeen, C. G., McInerney, J., Liu, H., Solomon, S. C., Polvani, L. M., Emmons, L. K., Lamarque, J., Richter, J. H., Glanville, A. S., Bacmeister, J. T., Phillips, A. S., … Randel, W. J. (2019). The Whole Atmosphere Community Climate Model Version 6 (WACCM6). Journal of Geophysical Research: Atmospheres, 124(23), Article 23.

Golaz, J.-C., Van Roekel, L. P., Zheng, X., Roberts, A. F., Wolfe, J. D., Lin, W., et al. (2022). The DOE E3SM Model version 2: Overview of the physical model and initial model evaluation. Journal of Advances in Modeling Earth Systems, 14, e2022MS003156, https://doi.org/10.1029/2022MS003156

Gutjahr, O., Putrasahan, D., Lohmann, K., Jungclaus, J. H., von Storch, J.-S., Brüggemann, N., Haak, H., & Stössel, A. (2019). Max Planck Institute Earth System Model (MPI-ESM1.2) for the High-Resolution Model Intercomparison Project (HighResMIP). Geoscientific Model Development, 12(7), 3241–3281. https://doi.org/10.5194/gmd-12-3241-2019

Held, I. M., Guo, H., Adcroft, A., Dunne, J. P., Horowitz, L. W., Krasting, J., Shevliakova, E., Winton, M., Zhao, M., Bushuk, M., Wittenberg, A. T., Wyman, B., Xiang, B., Zhang, R., Anderson, W., Balaji, V., Donner, L., Dunne, K., Durachta, J., … Zadeh, N. (2019). Structure and Performance of GFDL's CM4.0 Climate Model. Journal of Advances in Modeling Earth Systems, 11(11), 3691–3727. https://doi.org/10.1029/2019MS001829

Kim, YoungHo; Noh, Yign; Kim, Dongmin; Lee, Myong-In; Lee, Ho Jin; Kim, Sang Yeob; Kim, Daehyun (2019). KIOST KIOST-ESM model output prepared for CMIP6 CMIP. Version YYYYMMDD[1].Earth System Grid Federation. https://doi.org/10.22033/ESGF/CMIP6.1922

Lin, Y., Huang, X., Liang, Y., Qin, Y., Xu, S., Huang, W., Xu, F., Liu, L., Wang, Y., Peng, Y., Wang, L., Xue, W., Fu, H., Zhang, G. J., Wang, B., Li, R., Zhang, C., Lu, H., Yang, K., … Gong, P. (2020). Community Integrated Earth System Model (CIESM): Description and Evaluation. Journal of Advances in Modeling Earth Systems, 12(8), e2019MS002036. https://doi.org/10.1029/2019MS002036

https://doi.org/10.5194/egusphere-2024-2744
Preprint. Discussion started: 3 April 2025

Lurton, T., Balkanski, Y., Bastrikov, V., Bekki, S., Bopp, L., Braconnot, P., Brockmann, P., Cadule, P., Contoux, C., Cozic, A., Cugnet, D., Dufresne, J.-L., Éthé, C., Foujols, M.-A., Ghattas, J., Hauglustaine, D., Hu, R.-M., Kageyama, M., Khodri, M., … Boucher, O. (2020). Implementation of the CMIP6 Forcing Data in the IPSL-CM6A-LR Model. Journal of Advances in Modeling Earth Systems, 12(4), e2019MS001940. https://doi.org/10.1029/2019MS001940

Massonnet, F., Ménégoz, M., Acosta, M., Yepes-Arbós, X., Exarchou, E., & Doblas-Reyes, F. J. (2020). Replicability of the EC-Earth3 Earth system model under a change in computing environment. Geoscientific Model Development, 13(3), 1165–1178. https://doi.org/10.5194/gmd-13-1165-2020

Mauritsen, T., Bader, J., Becker, T., Behrens, J., Bittner, M., Brokopf, R., Brovkin, V., Claussen, M., Crueger, T., Esch, M., Fast, I., Fiedler, S., Fläschner, D., Gayler, V., Giorgetta, M., Goll, D. S., Haak, H., Hagemann, S., Hedemann, C., … Roeckner, E. (2019). Developments in the MPI-M Earth System Model version 1.2 (MPI-ESM1.2) and Its Response to Increasing CO2. Journal of Advances in Modeling Earth Systems, 11(4), 998–1038. https://doi.org/10.1029/2018MS001400

Park, S., Shin, J., Kim, S., Oh, E., & Kim, Y. (2019). Global Climate Simulated by the Seoul National University Atmosphere Model Version 0 with a Unified Convection Scheme (SAM0-UNICON). Journal of Climate, 32. https://doi.org/10.1175/JCLI-D-18-0796.1

Seland, Ø., Bentsen, M., Olivié, D., Toniazzo, T., Gjermundsen, A., Graff, L. S., Debernard, J. B., Gupta, A. K., He, Y.-C., Kirkevåg, A., Schwinger, J., Tjiputra, J., Aas, K. S., Bethke, I., Fan, Y., Griesfeller, J., Grini, A., Guo, C., Ilicak, M., … Schulz, M. (2020). Overview of the Norwegian Earth System Model (NorESM2) and key climate response of CMIP6 DECK, historical, and scenario simulations. Geoscientific Model Development, 13(12), 6165–6200. https://doi.org/10.5194/gmd-13-6165-2020

Tang, Q., Golaz, J. C., Van Roekel, L. P., Taylor, M. A., Lin, W., Hillman, B. R., ... & Bader, D. C. (2023). The fully coupled regionally refined model of E3SM version 2: overview of the atmosphere, land, and river results. Geoscientific Model Development, 16(13), 3953-3995.

Tatebe, H., Ogura, T., Nitta, T., Komuro, Y., Ogochi, K., Takemura, T., Sudo, K., Sekiguchi, M., Abe, M., Saito, F., Chikira, M., Watanabe, S., Mori, M., Hirota, N., Kawatani, Y., Mochizuki, T., Yoshimura, K., Takata, K., O'ishi, R., … Kimoto, M. (2019). Description and basic evaluation of simulated mean state, internal variability, and climate sensitivity in MIROC6. Geoscientific Model Development, 12(7), 2727–2765. https://doi.org/10.5194/gmd-12-2727-2019

van Noije, T., Bergman, T., Le Sager, P., O'Donnell, D., Makkonen, R., Gonçalves-Ageitos, M., Döscher, R., Fladrich, U., von Hardenberg, J., Keskinen, J.-P., Korhonen, H., Laakso, A., Myriokefalitakis, S., Ollinaho, P., Pérez García-Pando, C., Reerink, T., Schrödner, R., Wyser, K., & Yang, S. (2021). EC-Earth3-AerChem: A global climate model with interactive aerosols and atmospheric chemistry participating in CMIP6. Geoscientific Model Development, 14(9), 5637–5668. https://doi.org/10.5194/gmd-14-5637-2021

Wyser, K., van Noije, T., Yang, S., von Hardenberg, J., O'Donnell, D., & Döscher, R. (2020). On the increased climate sensitivity in the EC-Earth model from CMIP5 to CMIP6. Geoscientific Model Development, 13(8), 3465–3474. https://doi.org/10.5194/gmd-13-3465-2020

https://doi.org/10.5194/egusphere-2024-2744
Preprint. Discussion started: 3 April 2025

Yukimoto, S., Kawai, H., Koshiro, T., Oshima, N., Yoshida, K., Urakawa, S., Tsujino, H., Deushi, M., Tanaka, T., Hosaka, M., Yabu, S., Yoshimura, H., Shindo, E., Mizuta, R., Obata, A., Adachi, Y., & Ishii, M. (2019). The Meteorological Research Institute Earth System Model Version 2.0, MRI-ESM2.0: Description and Basic Evaluation of the Physical Component. Journal of the Meteorological Society of Japan. Ser. II, 97(5), 931–965. https://doi.org/10.2151/jmsj.2019-051

Ziehn, T., Chamberlain, M. A., Law, R. M., Lenton, A., Bodman, R. W., Dix, M., Stevens, L., Wang, Y.-P., Srbinovsky, J., Ziehn, T., Chamberlain, M. A., Law, R. M., Lenton, A., Bodman, R. W., Dix, M., Stevens, L., Wang, Y.-P., & Srbinovsky, J. (2020). The Australian Earth System Model: ACCESS-ESM1.5. Journal of Southern Hemisphere Earth Systems Science, 70(1), 193–214. https://doi.org/10.1071/ES19035